RSC Advances

PAPER

View Article Online
View Journal | View Issue

Cite this: *RSC Adv.*, 2021, **11**, 6825

Adsorption of CO_2 on the ω-Fe (0001) surface: insights from density functional theory

S. Assa Aravindh, *[a] Wei Cao, [a] Matti Alatalo,[a] Marko Huttula[a] and Jukka Kömi[b]

The stabilization of a hexagonal phase known as the ω-phase in steel has recently been identified. The presence of C in steel samples is found to be helping the formation of this otherwise meta stable phase. This indicates that the probability of degradation of the surface is high in steel samples containing the ω-phase, through surface adsorption. Here we calculate the adsorption process of CO_2 on the ω-Fe(0001) surface, for different sites and find that it strongly adsorbs horizontally with a bent configuration. The adsorption is characterized by significant charge transfer from the surface Fe atoms to the CO_2 molecule, and structural modification of the molecule is occurring. The density of states calculations indicate that hybridization and subsequent charge transfer is probable between the d orbitals of Fe and p orbitals of CO_2, resulting in strong chemisorption, that further leads to spontaneous dissociation of the molecule.

Received 28th October 2020
Accepted 29th January 2021

DOI: 10.1039/d0ra09194d

rsc.li/rsc-advances

1 Introduction

A hexagonal phase, known as omega (ω) has been identified in transmission electron microscopy (TEM) measurements in steel samples.[1–12] The ω phase is supposed to be metastable, yet getting trapped in crystal defects and it has been shown that the stabilization of ω occurs as an intermediate phase between the bcc–fcc transition in steel[7] and the presence of C is known to influence its formation. Ping *et al.*[1] have shown that the ω phase possesses 3.6% lower volume and 0.18 eV per cell higher energy than bcc-Fe, with atoms in alternate layers coupling antiferromagnetically. The increase in C concentration is found to assist in the stabilization of the ω phase and at higher concentrations, it will be stabilized as ω-Fe_3C. This hexagonal phase often acts as a sink for vacancies and impurities such as H or He atoms. In this scenario, the probability of CO_2 corrosion in steel, aided by the presence of the ω phase and dissolved CO_2 is highly probable, and that will be detrimental to many industries.[13] The mechanisms underlying CO_2 corrosion consist of many mechanical and environmental factors.[14] Temperature is one of the prominent factors in CO_2 corrosion, as it affects the formation of a protective layer. Hence, the possibility of formation of a protective layer is lower in omega-Fe surfaces as this meta stable structure is often formed due to mechanical constraints at grain/twin boundaries.[6] The ω-phase forms mostly at interfaces or twin boundaries in steel in the presence of atomic constraints,[6] which was earlier attributed to extra electron diffraction spots arising from internal twins or carbides. Another important factor influencing the formation of ω is the presence of C in steel.[1,7,8] Since the ω-phase is found to be formed at the interfaces and boundaries, exposure to gases and contaminants is higher than that of the bulk part of the material. Hence the possibility of CO_2 induced corrosion is highly probable in this meta stable phase and present investigation focus on the energetic of CO_2 adsorption on ω-Fe surfaces. It has been reported that the presence of CO_2 combined with moisture exposure can lead to formation of carbonic acid and cause corrosion in steel pipe lines.[15] Hence it is important to investigate the stability and structural changes caused by the adsorption of CO_2 as well as the possibility of activation of the C=O bonds, that leads to dissociation. In this scenario, we employ density functional theory (DFT) to investigate the adsorption energy, electronic structure and quantify the charge transfer properties of CO_2 on ω surface. Our results provide useful insights into the CO_2 dissociation mechanism at the ω-Fe surface, since we have seen that the activation of the molecule occurs at the surface followed by dissociation, due to the strong charge transfer between surface and adsorbates. This indicates that compared to the more inert CO_2 molecule, the CO moiety can interact with atmospheric moisture and enhance the degradation of the surface.

2 Computational methodology

The DFT calculations are carried out using plane wave-based pseudopotential code Vienna *Ab initio* Simulation Package (VASP).[16–18] A kinetic energy cut-off of 520 eV is used to expand the plane waves included in the basis set. Spin polarization is included in the calculations with Gaussian smearing and a smearing width of 0.01 eV is used.[19] The ω-Fe(0001) surface is

[a]*Nano and Molecular Systems Research Unit, University of Oulu, FIN-90014, Finland*
[b]*Materials and Mechanical Engineering Research Unit, University of Oulu, FIN-90014, Finland. E-mail: Assa.Sasikaladevi@oulu.fi*

modeled using the optimized atomic coordinates of a unit cell of $(1 \times 1 \times 1)$ ω-Fe. The optimized lattice parameters for the ω-Fe unit cell are $a = 3.85$ Å and $c = 2.42$ Å, and are in agreement with previously reported values.[1] To construct a surface slab, vacuum layers are added along the z-direction to make the interaction between the periodically repeated images negligible. The supercell dimensions are $a = 7.94$ Å, $b = 7.94$ Å and $c = 17.18$ Å respectively such that 36 Fe atoms are present. For the integration of the Brillouin zone, a Gamma centered k grid of $(5 \times 5 \times 2)$ dimensions is used. The ω-Fe(0001) surface is relaxed without symmetry constraints such that corresponding energy and force tolerances of 10^{-6} eV and 0.001 eV Å^{-1}, respectively, are achieved. The exchange and correlation is described using generalized gradient approximation (GGA). We employ the projected augmented wave method (PAW) in the parameter-free Perdew–Burke–Ernzerhof (PBE) formalism.[19,20] The above choices are based on previous studies that have shown that the PBE approximation accurately reproduces the energetic and magnetic properties of Fe based systems and specifically those of ω-Fe in the presence of alloying elements.[1,5,21] Initially we optimized the slab supercell relaxing all layers and upon addition of CO_2 molecule, bottom layers are fixed to bulk positions and top layers are relaxed.

The adsorption energy of CO_2 on the ω-Fe (0001)surfaces is calculated using the relation,[22]

$$E_{ads} = E_{surf+CO_2} - E_{surf} + E_{CO_2} \quad (1)$$

where E_{surf} is the total energy of the pristine ω-Fe (0001) surface slab, and $E_{surf+CO_2}$ is the total energy of the ω-Fe(0001) surface slab with CO_2 molecule adsorbed on it. The energy of the CO_2 molecule is calculated as the energy obtained by putting the CO_2 molecule in a cubic unit cell of size 20 Å followed by optimization. For the configurations in which CO_2 spontaneously dissociates to O and CO, the chemical potential of O atom and CO molecule, calculated using the cubic super cell approach is used for the adsorption energy calculations. From this equation, it turns out that a negative value of E_{ads} means exothermic reaction and thermodynamically favorable adsorption process while a positive value of E_{ads} indicates an endothermic reaction.

3 Results and discussion

The optimized geometry and orbital resolved density of states of ω-Fe (0001) are shown in Fig. 1(a) and (b) respectively. The density of states is metallic and dominated by the contribution from Fe-*d* orbitals surrounding the Fermi level. This indicates that the chances of hybridization of Fe-*d* orbitals and *p*-orbitals of the CO_2 molecule are highly probable. After the pristine surface is optimized, CO_2 molecule is placed on the surface and the adsorption energies are calculated after optimization. It is worthwhile to mention that to model the adsorption of CO_2 with the Fe surface, both the atoms of CO_2 and three topmost layers of the slab are subjected to unconstrained relaxation, such that the residual forces on all atoms reached 0.001 eV Å^{-1}. Furthermore, no symmetry constraints are imposed during the structural optimization; and the CO_2 molecule was free to move laterally and vertically from the initial site as well as to reorient itself to the minimum energy geometry. Total 8 configurations were considered including both vertical and horizontal orientations of CO_2. The configurations are chosen in such a way that, the vertical CO_2 perpendicularly aligned above the top of an Fe atom, attached over an Fe–Fe bond, attached in the hollow space formed by three Fe atoms situated at the three corners of a triangle and also on top of an Fe atom in the middle of the hexagonal ring. Same configurations were considered for the horizontal alignment of CO_2. The stable adsorption geometries after relaxation are presented in Fig. 2. The perpendicularly oriented linear CO_2 configurations (d), (e) and (f) present very weak adsorption with the omega surface, indicating a physisorption, evident from the longer Fe–O distances. The adsorption energies are positive in these three cases, indicating that the reaction is endothermic.

The linear configuration (a) on the other hand, spontaneously dissociates into O and C═O species with adsorption energy of −3.64 eV. For the configurations (a) and (g) a spontaneous CO═O bond cleavage is occurring, indicating that the dissociation process occurs without an energy barrier. The configurations (c) and (h) showed the lowest adsorption energies for CO_2 adsorption. Both (c) and (h) are almost equivalent positions geometrically, where CO_2 adsorbs in a bent configuration whereby the C and O atoms are adsorbed on top of nearby Fe atoms constituting the hexagonal ring on the surface. The calculated bond lengths are presented in Table 1. Though the bond lengths are almost similar between the two configurations, the O–C–O bond angles are 124.22 degree for (c) and 129.32 degree for (h) respectively. The lower bond angle for the configuration (c) indicates that the molecule is activated more in this case. The chemisorption of CO_2 on the ω-Fe(0001) surface in turn affects the C–O bond strength, and consequently, the possibility of decomposition of CO_2 moiety into surface bound oxygen and CO is possible. It can be seen that the C–O bonds for the configurations with least adsorption energy are elongated to 1.29–1.34 Å, compared to the gas phase C–O bond length which is 1.17 Å signifying that the C–O bonds are activated. For the most stable configurations adsorbed through chemisorption, it can be seen that the CO_2 adsorb in a bent configuration such that CO_2 molecule interacts with two surface Fe atoms through both oxygen atoms. The extended C–O bond lengths signify that these bonds are weakened due to the π-antibonding occupation, which may further lead to activation of the molecule, and help in the reduction of the CO_2 molecule on the surface. It can be seen that in the chemisorbed configurations, all the atoms share bonds with the substrate Fe atoms. Further, since the CO_2 molecule can receive electrons into the lowest unoccupied molecular orbital to become negatively charged bent species, the charge transfer between atoms are calculated.

Bader charge analysis was carried out[23,24] to quantify the charge transfer mechanism between the surfaces and CO_2. The calculated values are shown in Table 1. It can be seen that there exist significant charge transfer between the Fe surface and the C, O atoms for the chemisorbed configurations. The negative charge on the O atoms indicate that electrons are gained,

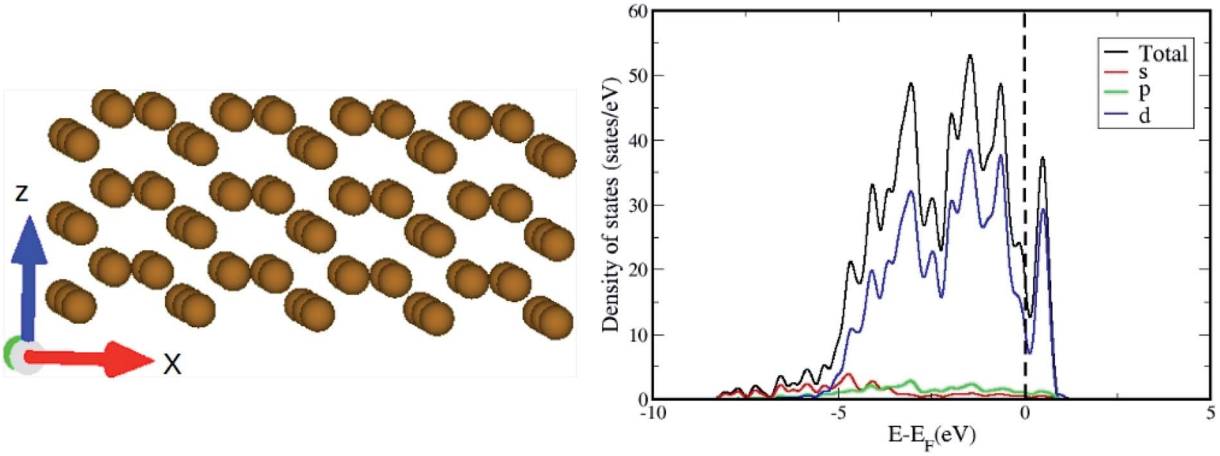

Fig. 1 (a) The optimized geometry and (b) the density of states of ω-Fe (0001) surface.

results in a net charge gain as CO_2 molecule. For the most stable CO_2 adsorbed configuration (c), while the C atom and Fe atoms bonded to C and first O atom lose charge, the Fe atom bonded to the second O atom, slightly gains charge. For the three physisorbed configurations (d), (e) and (f), there is no change in charge of the C atom. While the C atom is attached to the Fe

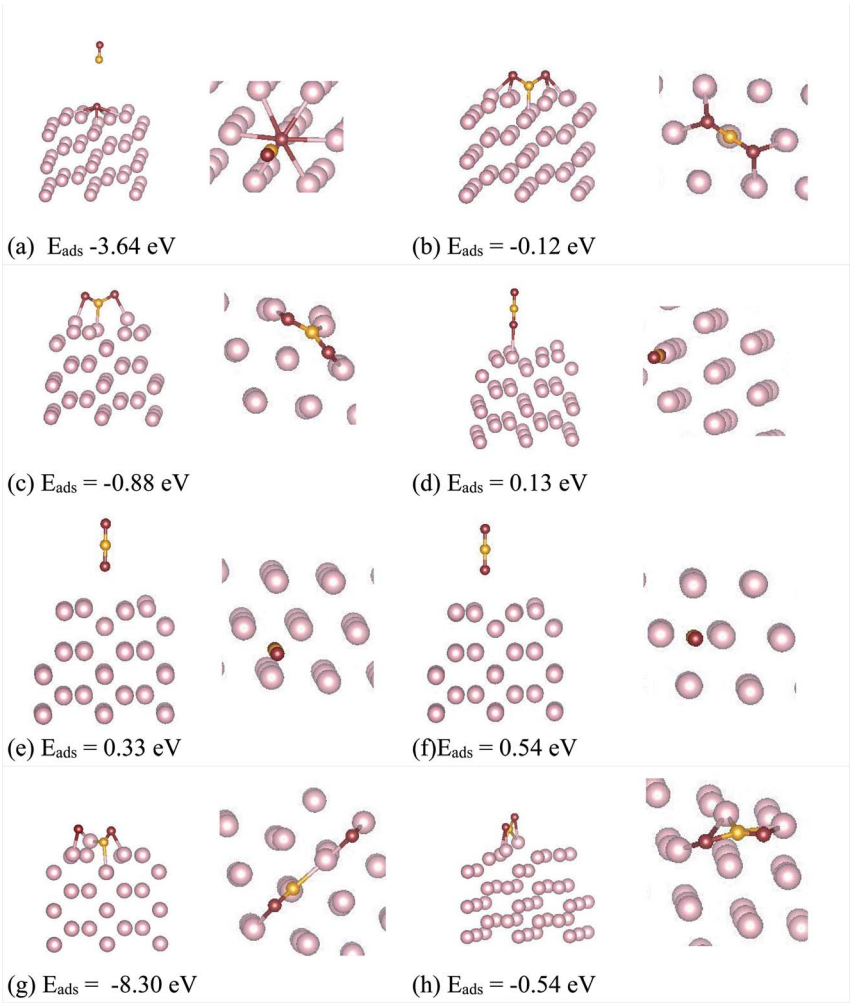

Fig. 2 The relaxed configurations of CO_2 over ω-Fe(0001) surfaces are presented in configurations a–h. The side and top views are shown. The color code of the atoms are, light pink – Fe, yellow – C and red – O respectively.

Table 1 The table shows relaxed bond lengths and Bader charges of the CO_2 on ω-Fe(0001) surface. For the Bader charges, the atom bonded with Fe is shown in parenthesis

	Relaxed bond lengths (Å)					Bader charges					
Configuration	d(C–O_1)	d(C–O_2)	d(Fe–O_1)	d(Fe–O_2)	d(Fe–C)	O_1	O_2	C	Fe(C)	Fe(O_1)	Fe(O_2)
(a)	3.63	1.14	1.87			−1.04	−1.83	1.83		0.34	
(b)	1.34	1.34	2.07	2.07	1.93	−1.71	−1.71	1.94			
(c)	1.29	1.29	1.97	1.93	1.97	−1.74	−1.72	2.38	0.10	0.14	−0.01
(d)	1.18	1.17	2.37			−2.07	−1.98	4		0.14	
(e)	1.18	1.18	2.72			−2.02	−2.04	4			
(f)	1.18	1.17	2.76			−2.03	−2.01	4			
(g)	5.24	1.30	2.96	1.79	1.97	−1.84	−1.01	0.61	0.37	0.28	0.24
(h)	1.29	1.27	1.99	2.05	1.97	−1.81	−1.72	2.44	0.09	−0.05	−0.17

atom at the center of the hexagonal ring, the detached O atom moves to a nearest neighbor Fe atom, such that the O atoms acquire charges, and C and Fe atoms loose charge. For the configuration (g) where, the CO_2 dissociates to O and CO moieties, there is significant charge transfer between the C and O atoms. This combined with the elongated bonds establish the fact that the CO_2 molecule dissociates without energy barriers in this configuration.

We analyze the partial density of states (PDOS) projected onto molecular orbitals of the most stable configuration with CO_2 adsorption and presented in Fig. 3. As the DOS for all chemisorbed CO_2 configurations are not so different from each other, we have only shown the DOS for the most stable surface + CO_2 geometry. The PDOS calculated for the isolated CO_2 molecule, projected on to the p orbitals are also shown in Fig. 3. Owing to the chemisorption, the p orbitals of CO_2 shift downwards from the Fermi level, presenting strong overlap with the d orbitals of Fe, indicating strong interaction and chemisorption on the surface. We plot the density of states (DOS) projected on to the d orbital for a surface Fe atom for the pristine surface and for the most stable CO_2 adsorbed configuration in Fig. 4. The Fe site is the one where the C atom is attached to form a Fe–C bond, such that the changes in d band can be analyzed before and after adsorption. It can be seen that the density of states of the Fe atom shift towards the Fermi level after adsorption of the CO_2 molecule, indicating the strong adsorption. The p orbitals of CO_2 can effectively hybridize with the d orbitals of the Fe surface, creating strong Fe–C and Fe–O bonds with the bent CO_2 molecule making significant charge transfer from the Fe d orbitals in to the p orbitals of CO_2 molecule results in the formation of a negatively charged CO_2 species as evidenced by the Bader charge analysis. This strong charge transfer is related to the elongation of the C–O bond, resulting in its activation.

To get deeper understanding of the charge redistribution at the ω-Fe(0001) surface caused by the CO_2 adsorption, we have calculated the charge density difference. It is calculated by subtracting the sum of the charge densities of the CO_2 molecule and the pristine ω-Fe(0001) surface, from the charge density of the adsorbate–substrate system. The charge density difference is calculated for the most stable CO_2 adsorption configuration

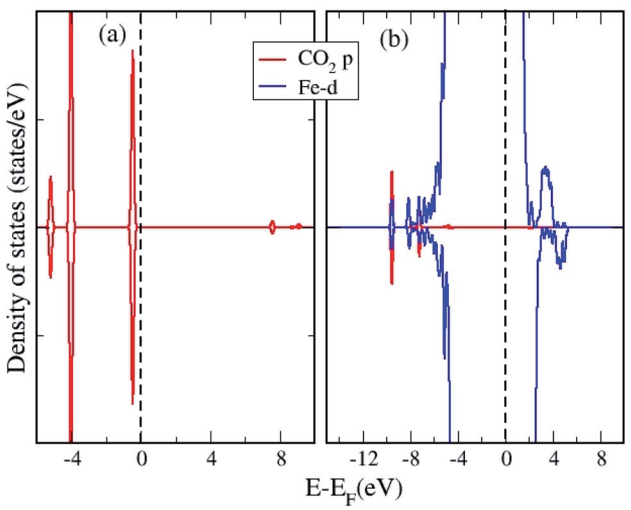

Fig. 3 The orbital projected density of states of (a) isolated CO_2 molecule and (b) ω-Fe(0001) surface with chemisorbed CO_2 molecule.

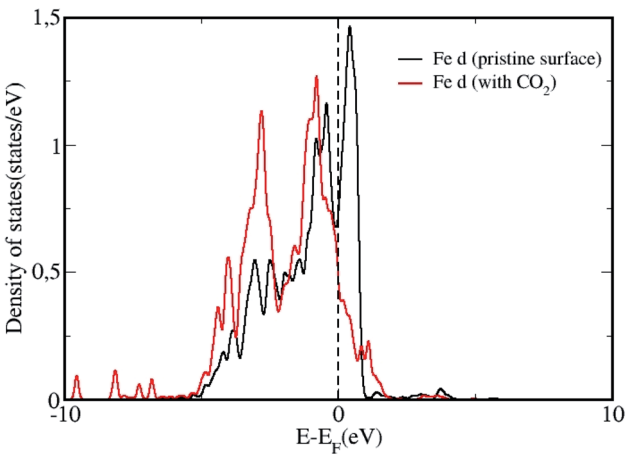

Fig. 4 The d orbital resolved density of states of an Fe atom at the ω-Fe(0001) surface before after adsorption of CO_2. The Fe atom correspond to the most stable adsorbed configuration of CO_2 adsorption and forms the Fe–C bond.

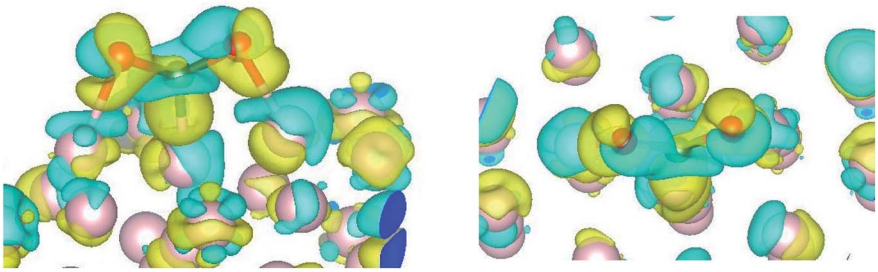

Fig. 5 The charge density difference plot of CO_2 adsorption on ω-Fe(0001) surface showing charge transfer in the regions between the CO_2 and the surface Fe atoms upon adsorption. The isosurface level is 0.0467125 electrons per $Å^3$. The yellow and blue regions indicate charge depletion and accumulation respectively. Figures (a) and (b) show the side and top view for the charge density difference calculated for the most stable configuration.

and shown in Fig. 5. It can be seen that all the three Fe atoms directly bonded to the CO_2 molecule presents charge depletion, which is extended towards the Fe–O and Fe–C bonds. The O atoms are surrounded by fractions of negative charge. The positive and negative charges are plotted with the same isosurface level. It can be seen from the figure that significant charge rearrangement happens only at the surface Fe layers. There is significant charge depletion from the Fe atoms and charge gain by the O atoms, and the positive charge is accumulated towards the Fe–C and Fe–O bonds. The significant charge transfer is evidenced by the Bader charge, that helps in strong chemisorption and further dissociation of the molecule. This indicates that compared to the inert CO_2, CO can stay at the surface, interacting with other species and enhance the degradation of the Fe surface.

4 Conclusions

We have carried out a study of the adsorption of CO_2 on ω-Fe(0001) surface. Among the 8 configurations considered, a horizontal bent configuration attaches with the least adsorption energy. It is observed that the CO_2 molecule is getting activated when attached in the horizontal bent configuration and dissociates spontaneously without an energy barrier. Strong charge transfer is noticed between the adsorbed CO_2 atom and the surface Fe atoms, which is further quantified from Bader charge analysis and charge density difference plots. The possibility of charge transfer from Fe d orbitals to p orbitals of CO_2 molecule is confirmed from the density of states, which aids in its stabilization at the surface. Our study provides important insights into the possibility of stabilization and dissociation of CO_2 on ω-Fe surface, which is important in the context of degradation aspects of Fe surfaces.

Funding information

The funding of this research activity is under the auspices of the Genome of Steel (Profile3) by the Academy of Finland through project #311934.

Research resources

The CSC – IT Center for Science, Finland.

Conflicts of interest

The authors declare no conflict of interest.

References

1 D. H. Ping and W. T. Geng, *Mater. Chem. Phys.*, 2013, **139**, 830–835.
2 T. Liu, D. Zhang, Q. Liu, Y. Zheng, Y. Su, X. Zhao, J. Yin, M. Song and D. Ping, *Sci. Rep.*, 2015, **5**, 15331.
3 P. D. Frost, W. M. Parris, L. L. Hirsch, J. R. Doig and C. M. Schwartz, *Trans. ASME*, 1954, **46**, 231–256.
4 B. S. Hickman, *J. Mater. Sci.*, 1969, **4**, 554–563.
5 Y. Ikeda and I. Tanaka, *Phys. Rev. B*, 2016, **93**, 094108.
6 Y. Ikeda and I. Tanaka, *J. Alloys Compd.*, 2016, **684**, 624–627.
7 A. Togo and I. Tanaka, *Phys. Rev. B: Condens. Matter Mater. Phys.*, 2013, **87**, 184104.
8 S. Q. Wu, D. H. Ping, Y. Yamabe-Mitarai, W. L. Xiao, Y. Yang, Q. M Hu, G. P. Li and R. Yang, *Acta Mater.*, 2014, **62**, 122–128.
9 D. H. Ping and M. J. Ohnuma, *J. Mater. Sci.*, 2018, **53**, 5339–5355.
10 Y. K. Vohra, S. K. Sikka and R. Chidambaram, *J. Phys. F: Met. Phys.*, 1979, **9**, 1771.
11 D. H. Ping, H. P. Xiang, H. Chen, L. L. Guo, K. Gao and X. Lu, *Sci. Rep.*, 2020, **10**, 6081.
12 A. A. S. Devi, S. Pallaspuro, W. Cao, M. Somani, M. Alatalo, M. Huttula and J. Kömi, *Int. J. Quantum Chem.*, 2020, **120**, e26223.
13 J. B. Sun, G. A. Zhang, W. Liu and M. X. Lu, *Corros. Sci.*, 2012, **57**, 131–138.
14 S. D. Zhu, A. Q. Fu, J. Miao, Z. F. Yin, G. S. Zhou and J. F. Wei, *Corros. Sci.*, 2011, **53**, 3156–3165.
15 A. Pfennig and A. Kranzmann, *Corros. Sci.*, 2012, **65**, 441–452.
16 G. Kresse, *J. Non-Cryst. Solids*, 1995, **192**, 222–229.
17 G. Kresse and J. Furthmüller, *Comput. Mater. Sci.*, 1996, **6**, 15–50.

18 G. Kresse and J. Daniel, *Phys. Rev. B: Condens. Matter Mater. Phys.*, 1999, **59**, 1758.
19 A. De Vita, PhD thesis, Keele University, 1992, A. De Vita and M. J. Gillan, preprint, 1992.
20 P. E. Blöchl, *Phys. Rev. B: Condens. Matter Mater. Phys.*, 1994, **50**, 17953.
21 J. P. Perdew, K. Burke and M. Ernzerhof, *Phys. Rev. Lett.*, 1996, **77**, 3865.
22 S. Assa Aravindh, W. Cao, M. Alatalo and M. Huttula, *Appl. Surf. Sci.*, 2020, **512**, 146019.
23 G. Henkelman, A. Arnaldsson and H. Jónsson, *Comput. Mater. Sci.*, 2006, **36**, 354–360.
24 R. F. W. Bader, *Atoms in Molecules: A Quantum Theory*, Oxford University Press, London, 1994.